applied sciences

MDPI

Article

Landslide Susceptibility Using Climatic–Environmental Factors Using the Weight-of-Evidence Method—A Study Area in Central Italy

Matteo Gentilucci *, Niccolò Pelagagge, Alessandro Rossi, Aringoli Domenico and Gilberto Pambianchi

School of Sciences and Technologies, Geology Division, University of Camerino, 62032 Camerino, Italy
* Correspondence: matteo.gentilucci@unicam.it

Abstract: The Italian territory is subject to a high level of hydrogeological instability that periodically results in the loss of lives, buildings and productive activities. Therefore, the recognition of areas susceptible to hydrogeological instability is the basis for preparing countermeasures. In this context, landslide susceptibility in the mid-Adriatic slope was analyzed using a statistical method, the weight of evidence (WoE), which uses information from several independent sources to provide sufficient evidence to predict possible system developments. Only flows, slides, debris flows and mud flows were considered, with a total of 14,927 landslides obtained from the IFFI (Inventory of Franous Phenomena in Italy) database. Seven climatic–environmental factors were used for mapping landslide susceptibility in the study area: slope, aspect, extreme precipitation, normalized difference vegetation index (NDVI), CORINE land cover (CLC), and topographic wetness index (TWI). The introduction of these factors into the model resulted in rasters that allowed calculation by GIS-type software of a susceptibility map. The result was validated by the ROC curve method, using a group of landslides, equal to 20% of the total, not used in the modeling. The performance of the model, i.e., the ability to predict the presence or absence of a landslide movement correctly, was 0.75, indicating a moderately accurate model, which nevertheless appears innovative for two reasons: the first is that it analyzes an inhomogeneous area of more than 9000 km^2, which is very large compared to similar analyses, and the second reason is the causal factors used, which have high weights for some classes despite the heterogeneity of the area. This research has enabled the simultaneous introduction of unconventional factors for landslide susceptibility analysis, which, however, could be successfully used at larger scales in the future.

Keywords: landslide; susceptibility; TWI; AUC; NDVI; weight of evidence; WoE

Citation: Gentilucci, M.; Pelagagge, N.; Rossi, A.; Domenico, A.; Pambianchi, G. Landslide Susceptibility Using Climatic–Environmental Factors Using the Weight-of-Evidence Method—A Study Area in Central Italy. *Appl. Sci.* **2023**, *13*, 8617. https://doi.org/10.3390/app13158617

Academic Editor: Martín Jesús Rodríguez-Peces

Received: 4 July 2023
Revised: 21 July 2023
Accepted: 24 July 2023
Published: 26 July 2023

1. Introduction

The Italian territory is hydrogeologically rather fragile, due to its geological, geomorphological and hydrographic characteristics, which make it predisposed to landslide and flood risks. Italy is among the European countries most exposed to the danger of landslides, with 620,808 landslides registered, affecting 23,700 km^2 of territory, or 7.9% of the national territory [1]. In this context, countermeasures are needed that can contribute to the reduction in the landslide risk, through a correct assessment of even those areas that have not shown hydrogeological instability in recent times, but may still be affected by it. In particular, landslide susceptibility measures the probability that a landslide may occur in a given area, without taking into account the time factor that is decisive for the evaluation of landslide hazard [2]. Over the years, the scientific literature, through successive research, has isolated three types of processes common to each susceptibility map, firstly the creation of a model, secondly the choice of factors, and finally the validation of the method used in order to understand its performance [3]. The spatial processes for creating the map and obtaining the results for each factor are usually achieved through

GIS-type software [4]. With regard to the model used or the creation of the model itself, many possibilities have been explored by researchers around the world, but these can be grouped into two categories: statistical methods and deterministic methods [5]. Deterministic methods are based on precise mathematical laws, they are the simplest, the variables assume fixed values, these models can take the effect of chance into account to a certain extent; however, they are always deterministic in that the uncertainty associated with the input variables is not taken into account [6]. Deterministic quantitative methods depend on engineering principles of slope instability expressed in terms of the factor of safety [7]; due to the need for exhaustive in situ data from individual slopes, these methods are often effective for mapping only small areas [8]. Among deterministic methods, one method used with some success in southern Italy, in Calabria, has been Transient Rainfall Infiltration and Grid-based Slope-Stability (TRIGRS), in which physical–mechanical factors of soils (unit weight, cohesion, friction angle, soil depth, etc.) are introduced, very often on the basis of existing literature in the area [9]. Another interesting model but one that does not give particularly robust results is the shallow landslide stability model (SHALSTAB), which is a deterministic model used to produce shallow landslide susceptibility maps; the SHALSTAB model is based on two assumptions, on the one hand the stability of an infinite slope with a mobilizing cover on a stable basement, the output of the model is the critical heights of the shallow landslide that generate instability [10]. Sometimes, in order to improve the reliability of these deterministic models based on physical–mechanical factors, statistical methods are also used to give a probabilistic value to the analysis, learning from the experience of previous landslides. This is the case, for example, of a research conducted in Korea, which combined the deterministic SHALSTAB model with the spatial multi-criteria evaluation model (SMCE), which is a semi-quantitative model and produced rather high success rates of close to 80% [11]. Statistical methods operate very differently from deterministic methods, as they aim to correlate information on past landslide phenomena with a set of factors that are assumed to be directly or indirectly responsible for the propensity to trigger landslides and their consequences [12]. These methods are based on the relationships existing between landslide phenomena and predisposing factors of instability, through the attribution of weights that reflect the influence that each of these have on slope stability/instability [13,14]. In the case of statistical methods, therefore, it is sufficient to map the disasters that have occurred in order to be able to interpret them in the future by analyzing the factors that predisposed them. There are many statistical methods to assess slope instability, such as bivariate statistical analyses, logistic regressions, multiple linear regressions, fuzzy logic and neural networks [15]. An example of a bivariate statistics model is the Statistical Index, based on the correlation between landslides and prediction layers, but also the weight of evidence (WoE), which calculates the weight of each factor in terms of the presence or absence of landslides and then returns a contrast value; both of these have been found in the literature to have good prediction performance, particularly the WoE [16–18]. Logistic regression is probably the most widely used method in the study of landslide susceptibility. It involves the use of a binary variable (of the yes/no type) as the dependent variable and one or more variables, whether continuous or categorical, as the independent variables, and yields good results, in some cases correctly classifying more than 80% of the landslides [19]. As far as multiple linear regression is concerned, it is not among the most widely used methods, and as far as success rates are concerned, it is also not among the most consistent methods because the thresholds for discriminating between prediction of the presence of a possible landslide and prediction of its absence are rather subjective [20]. In fuzzy logic, on the other hand, there are many decisions that are left to the experience of the operator, with the result that performance can be variable and dependent on the choices made [21]. Neural networks currently represent the final frontier in the assessment of landslide susceptibility, having the ability to simulate brain connections and allowing through the technique of deep learning to learn from the layers used. There is a great deal of research that shows that artificial neural networks (ANNs) can predict landslide susceptibility very well compared to testing databases, reaching accuracies of

up to 90% [22]. However, the model is not the only discriminating factor in drawing up a landslide susceptibility map. In fact, the factors that are to be considered play a decisive role and are identified as predisposing factors whose weight is verified by entering them into the model. there are various types of factors that can be considered as triggering or predisposing factors for landslide movement, they can be topographic, hydrological, soil, geological, vegetation, land use or climatic factors [23–25]. While geology, topography and land use are the most commonly used variables for analyzing landslide susceptibility, others are less frequent and very often do not show clear correlations with landslide movements [26]. Some studies use the NDVI (normalized vegetation index) as the absence of vegetation can lead to less resistance to movement, others the TWI (Topographic Wetness Index), which calculates the moisture in the soil, and still others, although fewer in number, which consider extreme precipitation [27,28].

In the case of the present research, the aim of this study was to create a rather extensive landslide susceptibility map using climatic–environmental factors to understand their actual influence on slope stability, in a rather large area corresponding to the Adriatic slope in Central Italy. In this context, given the size of the area and the lack of in situ surveys, deterministic methods were discarded and a model based on statistical methods was chosen. Within these, the weight-of-evidence method has been shown by numerous studies to be one of the best performing methods in terms of prediction in discriminating the probability of landslide events spatially [29,30]. The WoE also in relation to more recently introduced methods, such as logistic regressions or artificial neural networks, generates very good results that lead to rather discordant opinions in the scientific literature, delineating a superiority of one or the other method depending on the different areas analyzed [31,32]. Therefore, for this study, it was decided to use the WoE for the model, incorporating climatic–environmental factors to take into account topography, geology, climate and vegetation. The objective was to evaluate the performance of the model, over a very large area such as the study area of more than 9000 square kilometers, across the area under the curve in an extremely heterogeneous topographical, climatic and environmental context, trying to make it an operational decision support tool.

2. Materials and Methods

2.1. Study Area and Database

The study area is located on the mid-Adriatic slope in central ltaly, in particular, the territory of the Marche Region was chosen (9344 km^2), an area that has never seen studies on its landslide susceptibility, but only in some cases very small portions of it have been analyzed. Marche Region is characterized by the total absence of flat areas of a certain extension, making it one of the most mountainous Italian regions; the average altitude is around 400 m (Figure 1) [33]. The associated plains are generally poorly developed, with the exception of the areas near the coast and in the areas close to the beds of the major rivers. In the northern portion of the territory, the Apennine chain is divided into two ridges: the inner Umbrian–Marchigiana ridge, which acts as a watershed between the Adriatic and Tyrrhenian rivers and is made up of the major reliefs, and the eastern Marche ridge. In terms of hydrography, the main rivers do not reach great lengths, only the Metauro and the Tronto exceed 100 km and all flow into the Adriatic Sea with estuaries, running in a W-SW to E-NE direction, only a few tributaries such as the Nera or the Torrente Ussita flow into the Tyrrhenian Sea [34]. Most of the sources of the main hydrographic drainage network (Foglia, Metauro, Esino, Chienti and Tronto) are located in the Umbro–Marchigiana ridge. In the mountainous portion, the valleys are narrow and deep mainly due to the action of linear erosion carried by the rivers (Figure 1) [35]. In the hilly section, there is a significant change in the morphology of the river valleys, which are wider and with ‘gentler’ slopes, dictated by the lower energy of the relief, resulting in less aggressive water action [36].

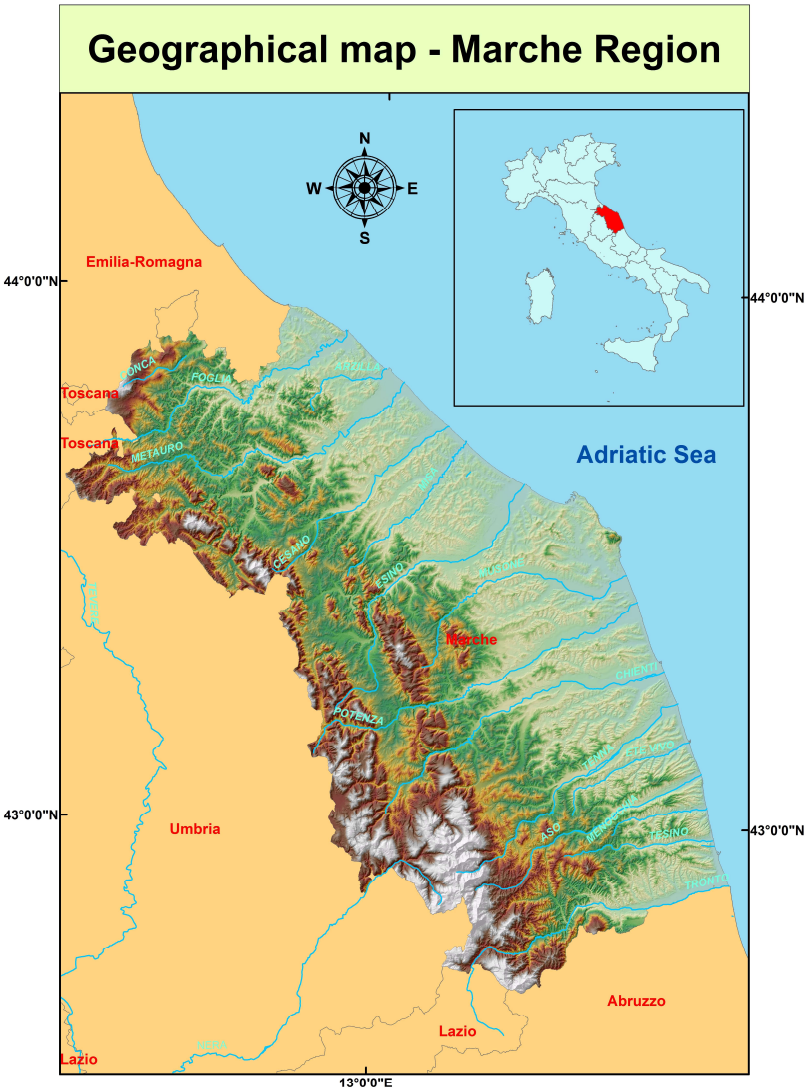

Figure 1. Geographical map of the Marche region [37].

As far as population is concerned, there are approximately 1.5 million people in this area, with a population density of 157 inhabitants per km^2, well distributed over most of the regional area, which makes it essential to find countermeasures to hydrogeological instability. From a geological point of view, the oldest outcrops consist of limestone and occupy the mountainous parts of the region; in the hilly areas, the sediments are calcareous, clayey, arenaceous and sometimes sandy or gravelly in composition, up to the Pliocene and, in part, Pleistocene sediments with sandy-clayey facies, with which the marine sedimentary cycle ends; Quaternary continental deposits were deposited at a later stage on soils that gradually emerged. Lastly, from a climatic point of view, we find ourselves in an area with a Mediterranean climate in the southern coastal part, a warm temperate climate in the central-northern coastal part, while then, continuing from east to west, we encounter temperate climates that are gradually colder, up to nival climates on the major Apennine peaks [38].

2.2. Database and Software

The database when using a statistical method of landslide susceptibility analysis is a fundamental part of this study. In particular, the landslide survey carried out by the Marche Region, through the Central Apennine District Basin Authority, was used in this study. In this context, the Hydrogeological Structure Plan (PAI), is configured as a functional outline of the hydraulic and hydrogeological hazard sector of the General Basin Plan. The file used for the analysis of landslide susceptibility was downloaded directly from the Marche region

website and contains all the data on landslide phenomena collected, classified according to type, activity, degree of risk and hazard. The gravitational phenomena selected are the movements of slides, flow, debris flow and mud flow, and 14,297 polygons were identified and used for the analysis (Figure 2). The visualization of the landslides, as well as the analyses were carried out in a GIS environment to obtain spatialized factors, calculating the topographical variables using a digital elevation model at 20 m obtained from the regional technical map.

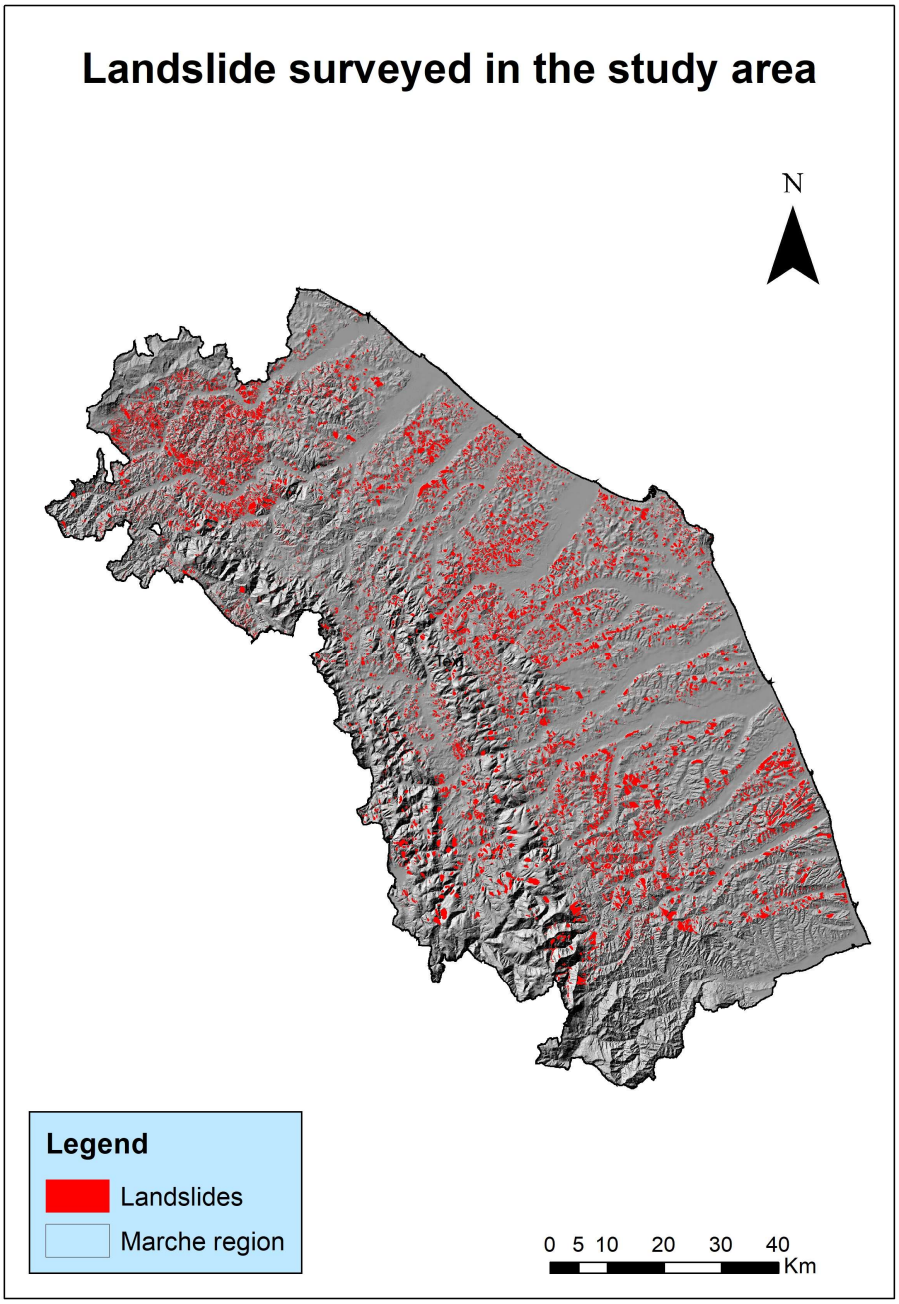

Figure 2. Distribution of landslides in the study area.

2.3. Statistical Model

The WoE is a quantitative method of combining evidence to support a hypothesis. The method was originally developed for applications in the medical field, in which symptoms were analyzed and from them the hypothesis regarding the patient's disease was obtained [39]; a pair of weights was calculated for each symptom, one for the presence

of the symptom and one for the absence of the symptom. The magnitude of the weights depended on the measured association between the symptom and the disease pattern in a large group of patients. The weights could then be used to estimate the probability of a new patient getting the disease, based on the presence or absence of symptoms. WoE were used in the late 1980s for mining research with GIS to obtain areas where the presence of deposits could be likely [40]. More recently, this method has also been applied to landslide susceptibility mapping [41]. Weights of evidence (WOE) is a Bayes rule-based approach to combine data and predict the occurrence of events, this method predicts the presence/absence of the event within a pixel and is based on deciding which state is most likely to occur based on the available data. The likelihood ratio technique aims to identify the degree of influence, expressed as a "weight", that each variable has on the development of a landslide event; the weights are calculated based on the spatial development of landslides in the thematic maps used as evidence. A positive weight (W^+) was calculated for each predictor variable when the event occurs and a negative weight (W^-) when the event does not occur; the weights are measures of correlation between the evidence (predictor variable) and the event. It is then possible to calculate the degree of influence that each factor has had, and will have in the future, on the development of landslide events. If a part of the studied area is affected by landslide phenomena $\left(A_f\right)$, the prior probability $\left(P_f\right)$ of finding a landslide within (A_t) (total area studied) is:

$$P_f = \frac{A_f}{A_t} \tag{1}$$

This initial estimate can increase or decrease depending on the relationships between the analyzed factors and the landslides. The probability (P_v) of finding one of the examined factors in the study area is given by:

$$P_v = \frac{T_v}{A_t} \tag{2}$$

where (T_v) = total area occupied by a certain factor class

$$W^+ = \ln\left(\frac{Landslide\ area\ in\ class/Total\ landslide\ area}{Stable\ area\ in\ class/Total\ stable\ area}\right) \tag{3}$$

$$W^- = \ln\left(\frac{Total\ landslide\ area\ outside\ class/Total\ landslide\ area}{Stable\ area\ outside\ class/Total\ stable\ area}\right) \tag{4}$$

The difference between W^+ and W^- provides insight into whether the analyzed factor is significant and influences the distribution of landslides in an area:

$$C = W^+ - W^- \tag{5}$$

where (C) = contrast.

A positive C-value emphasizes that the investigated feature has a greater weight, discriminating for the detection of possible landslides in the area, while a negative value represents a situation of greater stability of the investigated feature. On the other hand, when values are very close to zero, they have no significant influence in the model and the presence of that characteristic is not very indicative for landslide susceptibility.

The landslide susceptibility index (LSI) was calculated as follows (Figure 3):

$$LSI_C = C_{1st\ fac} + C_{2nd\ fac} + C_{3rd\ fac} + C_{4th\ fac} + C_{5th\ fac} + C_{6th\ fac} + C_{7th\ fac}$$

where ($C_{ist\ fac}$) = value of the contrast of each factor considered.

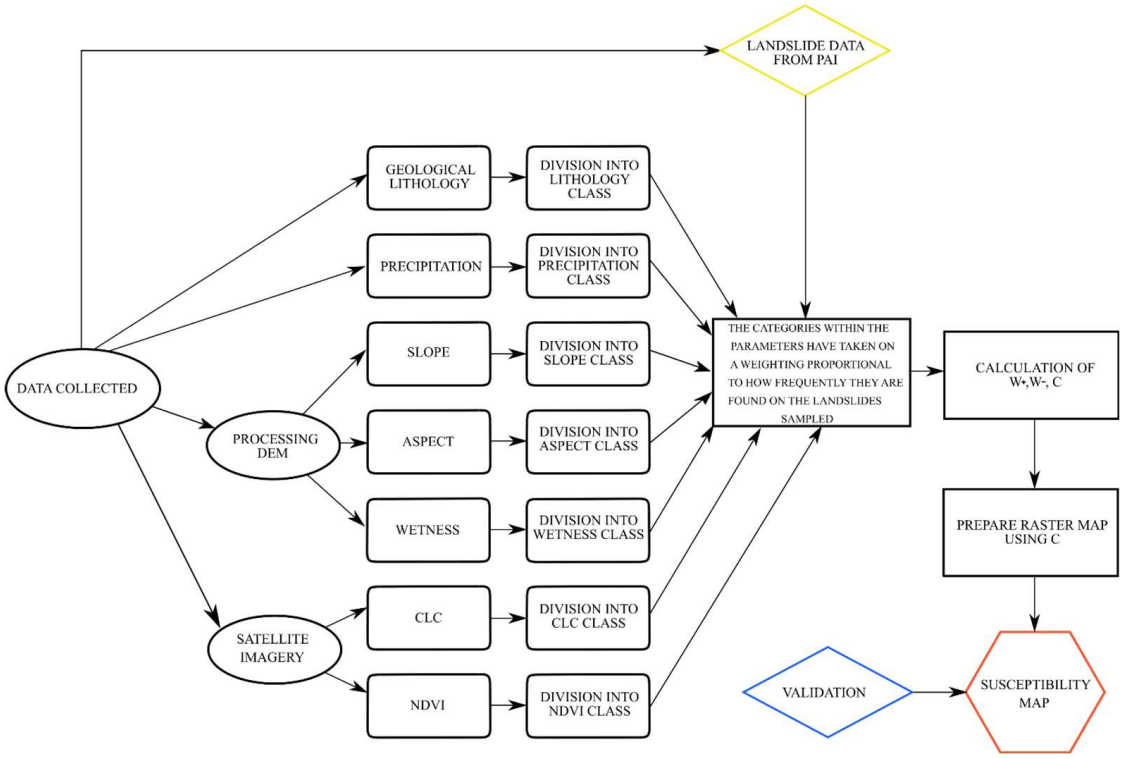

Figure 3. Model flow diagram.

2.4. Selected Landslide Causal Factors

The causal factors identified for this analysis were 7, some topographic and dem-derived, such as the aspect, slope and TWI (Topographic Wetness Index), the other climatic such as the analysis of extreme precipitation, then the geological one related to lithology, and finally two satellite factors, the CORINE land cover (CLC) and NDVI (normalized difference vegetation index).

Ten dip directions were considered to calculate aspect, in order to assess whether there is a particular exposure that statistically is more likely to trigger landslide movements, The appearance data have been reclassified into the following classes:

- Flat (0°),
- North (0–22.5°),
- Northeast (22.5–67.5°),
- East (67.5–112.5°),
- Southeast (112.5–157.5°),
- South (157.5–202.5°),
- Southwest (202.5–247.5°),
- West (247.5–292.5°),
- Northwest (292.5–337.5°), and
- North (337.5–360°).

The classification of the exposure was certainly very detailed with subdivisions according to the wind rose every 45° of inclination; however, it was interesting to have a more precise differentiation, also for future analyses. As for the slope, it was grouped into four groups from 0° to 16°, from 16° to 25°, from 25° to 35° and higher than 35°. Geologically, due to the characteristic friction angles of each debris, there is a certain dependence on the inclination of the topography, while the division into classes has been borrowed from other international research, which has shown a differential landslide triggering capacity for the specified values [42]. The TWI is an index used to measure how local topography controls local hydrological processes and shows the spatial spread of surface saturation

and soil moisture, in fact the following algorithm must show the impact of the local terrain on drainage [43]:

$$TWI = \ln\left(\frac{A}{\tan\beta}\right) \quad (6)$$

where A is the specific catchment area of a portion of land, where β is the slope angle.

It is common scientific knowledge that especially in the case of the landslide movements evaluated in this study, the imbibition of debris can increase the weight of the debris and allow the activation of a movement.

The following classes created on the basis of the TWI were chosen:

- 0–2,
- 2–4,
- 4–6,
- 6–8,
- 8–10,
- 10–12, and
- 12–23.

The classes were chosen using homogeneous differences between one and the other, with the last one being extended because for many of the values belonging to it, it is not sufficiently represented.

To spatially assess land use, the CLC updated to 2018 was used, thus with the measurements obtained from Sentinel-2, with the first level dividing the study area into the following homogeneous territories:

1. Artificial Surfaces,
2. Utilized Agricultural Areas,
3. Wooded Territories and Semi-Natural Environments,
4. Humid Zones (that are not present in the study area), and
5. Water Bodies.

The geology of the area, as in any susceptibility analysis, is very important, but equally fundamental is the aggregation between the various formations, on homogenous groups, in order to obtain a certain significance that would be lacking, especially over large areas where there may be many formations, due to the extreme fragmentation. The lithotypes have been grouped into the following hydrogeological classes [44]:

- Clays and marly clays with intercalations of sandstones, sands and conglomerates deposits;
- Deposits;
- Limestones, flinty limestones, subordinately marls and clay marls;
- Marls, clay marls and marly limestones;
- Sandstones, marly clays, subordinately conglomerates;
- Shales and marls encompassing calcareous, marly limestone and arenaceous bodies.

From the climatic point of view, an analysis of extreme precipitation on a regional scale was performed, with daily maximum precipitation data obtained through the "Regional Weather-Idro-Pluviometric Information System" database. 131 rain gauges in the most recent standard period 1991–2020 were taken into account; the data were then processed using the GEV (Generalized Extreme Values) technique and subsequently interpolated with GIS software. This led to the creation of a raster over the entire study area that allowed a detailed analysis of the influence of precipitation on landslide susceptibility.

There were eight classes obtained in this case:

- 100–115,
- 115–130,
- 130–145,
- 145–160,
- 160–175,
- 175–190,

- 190–205, and
- 205–250.

The NDVI is a vegetation index obtained from satellite images to assess the presence of photosynthetic activity. The index is calculated from satellite images produced by sensors that acquire in the red (R: 0.7 μm) and near-infrared (NIR: 0.9 μm). It assesses the presence of photosynthetic activity, as it relates the red spectrum, where there is absorption by chlorophyll, and the near-infrared spectrum where leaves reflect light to avoid overheating. The NDVI value ranges from −1 to 1, and the presence of vegetation takes values above 0.2 [45], and the formula for calculating the index is as follows:

$$NDVI = \frac{NIR - R}{NIR + R}$$

The classes created according to the NDVI value were divided into:

- no-vegetation (−1 to 0.199);
- low vegetation (0.2 to 0.5);
- high vegetation (0.501 to 1.0).

Aqua Moderate-Resolution Imaging Spectroradiometer (MODIS) Vegetation Indices (MYD13Q1) Version 6 data downloaded from the NASA website were generated every 16 days with a spatial resolution of 250 meters (m). The MYD13Q1 product provides the NDVI, indicated as a continuity index to the current NDVI derived from the National Oceanic and Atmospheric Administration-Advanced Very High Resolution Radiometer (NOAA-AVHRR).

2.5. Statistical Methods for Model Validation

Model validation is the last step in the landslide susceptibility mapping process and is used to assess reliability using statistical methods. It is important to define the accuracy of the model because a landslide susceptibility map without validation is meaningless in the scientific world [46]. In this case statistical method used was the ROC curve, originally developed during World War II to evaluate the capabilities of radar receivers in detecting targets, later also used in the medical field to perform diagnostic tests, and in machine learning [47,48]. The ROC curve (Receiver Operating Characteristic curve) is a graphical representation for evaluating the performance of a binary classification model that shows the relationship between the sensitivity (or true positive rate) and the specificity (false positive rate) of a test. The points on the ROC curve represent pairs of (false positive, true positive) derived from different contingency tables created by varying the boundary values. In relation to the occurrence of landslides, the sensitivity is calculated as follows:

$$y - axis,\ sensitivity = (TP/(TP + FN))$$

TP = true positive, FN = false negative, whereas specificity is described by the following formula:

$$x - axis,\ sensitivity = (FP/(FP + TN))$$

FP = false positive, TN = true negative.

In this context, true negatives represent the probability that a non-slide area is correctly detected by the LSI (Landslide Susceptibility Index); false positives, represent the probability that a landslide area will not be detected in relation to the LSI. On the other hand, true positives represent the probability that a landslide area is correctly classified in relation to LSI, while false negatives represent the probability that a 'non-landslide area' is incorrectly classified as a 'landslide area' with LSI. ROC curves can be quantitatively summarized using the area under the curve (AUC), measures the model's ability to discriminate between two classes (e.g., landslide and non-landslide) and provides a scale for assessing the overall quality of a model, the larger the AUC, the better the model's performance across the entire range of possible threshold values [49]. The area under the curve can take values between

0.5 and 1.0, the larger the area under the curve (i.e., the closer the curve is to the upper left-hand corner of the graph), the greater the discriminating power of the test. To interpret the values of the area under the ROC curve, one can refer to the following classification [50]:

- AUC = 0.5 the test is not informative;
- 0.5 < AUC $\leq$ 0.7 the test is inaccurate;
- 0.7 < AUC $\leq$ 0.9 the test is moderately accurate;
- 0.9 < AUC < 1.0 the test is highly accurate;
- AUC = 1 perfect test.

In the present work, 20% of the total landslides used in the calculation of the susceptibility map (training test) were used to validate the susceptibility map (Figure 4).

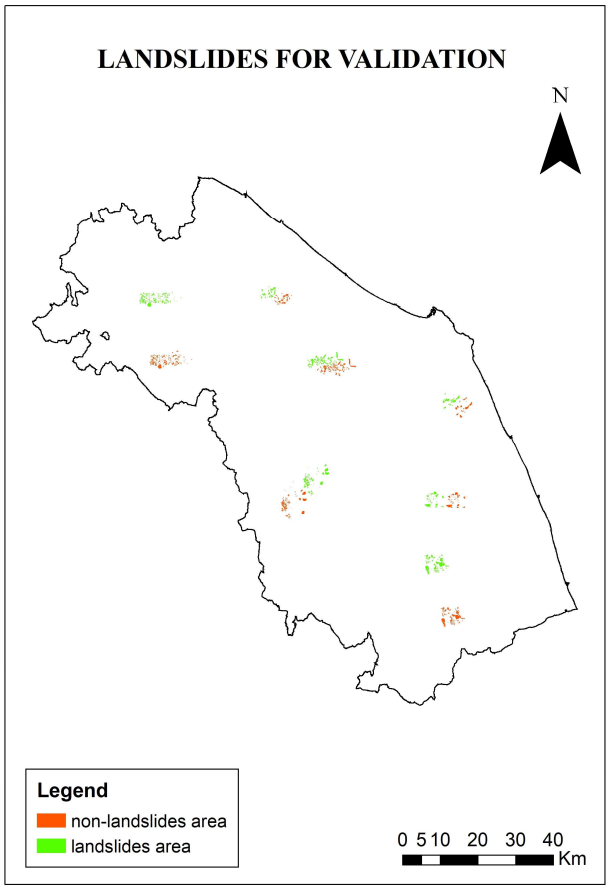

Figure 4. Map of landslide and non-landslide areas chosen for model validation.

Two polygons were created for the validation of landslides:

- the first file with the original landslide polygons then correctly georeferenced
- a second file with the landslide polygons deliberately shifted to create 'fake' landslide polygons to be used for the AUC calculation; this second file is crucial because a conservative model might detect landslide areas well, but mistake non-landslide areas for landslide areas.

3. Results

3.1. Causal Factors

Causal factors were counted spatially on the basis of the maps in Figure 2.

The maps of each causal factor were correlated with the landslides in the database in order to understand where the landslides fall and what their relationship is with the chosen causal factors (Figure 5).

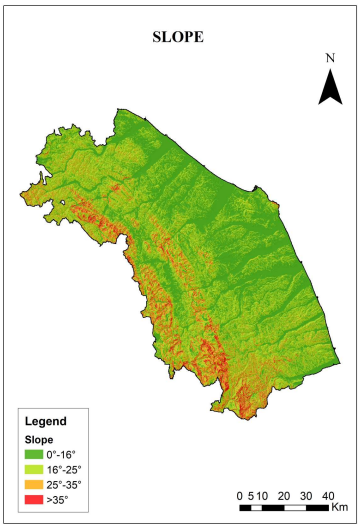

(**a**)

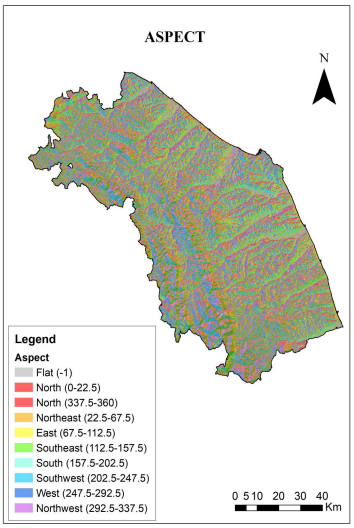

(**b**)

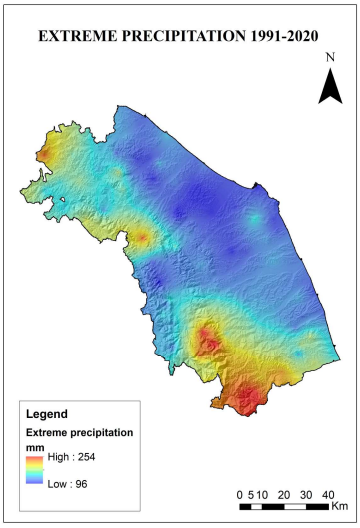

(**c**)

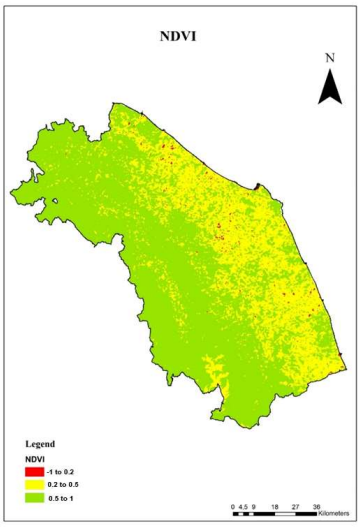

(**d**)

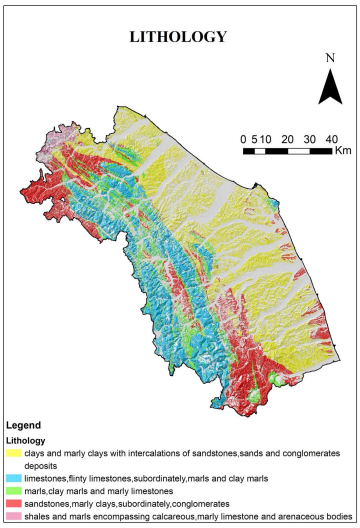

(**e**)

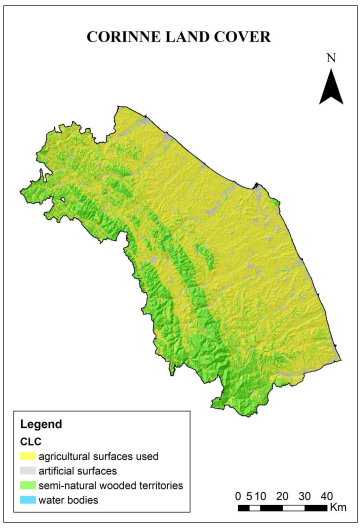

(**f**)

Figure 5. *Cont.*

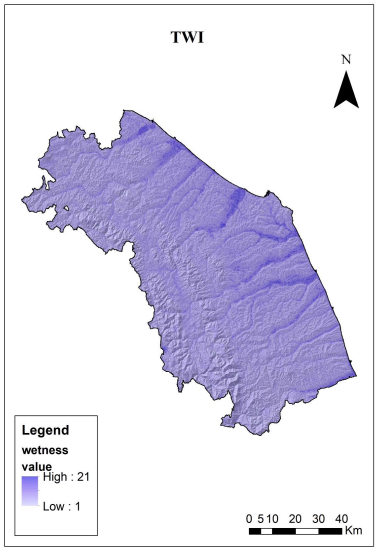

(**g**)

Figure 5. Maps of causal factors: (**a**) slope; (**b**) aspect; (**c**) extreme precipitation 1991–2020; (**d**) NDVI; (**e**) lithology; (**f**) CORINE land cover; (**g**) TWI.

Table 2 allows us to evaluate the contrast values for the various classes and some confirmations are highlighted, with predictable high or low values, but also with surprises that were not easy to expect. In particular, Table 2 tells us that the landslides studied are most frequently triggered at slopes of 16° to 25° and with a preferential exposure to the north, although to a lesser extent also to the northeast and northwest. However, where the area is flat or exposed to the south, the probability of having a landslide type flow, slides, debris flow or mud flow is much lower. As far as 24 h extreme precipitation is concerned, no very high correspondences are obtained, especially for the 100–115 mm, 130–145 mm and 145–160 mm classes, but this could have a rather interesting explanation. As in the mountainous area that is subject to the most intense 24 h precipitation, there are fewer accumulations of deposits and fewer areas subject to the landslides considered, so this probably explains the low significance for the most intense precipitation classes (205–250 mm). Then, considering the first satellite index investigated, we can see, as was to be expected, a greater likelihood of triggering landslide movements when the value is below 0.2, which identifies those areas where vegetation is absent and which do not provide sufficient protection from rainfall. Between 0.2 and 0.5, which identifies very lush low vegetation or sparsely lush high vegetation, the value decreases significantly and therefore landslides are not very likely to be triggered. The probability value of triggering a landslide movement decreases even more with NDVI values between 0.5 and 1, which are usually healthy shrubs and forests. The lithology shows that the only C that can give a probability of a landslide event occurring, is that of the areas above the deposits. Finally, the CLC showing a positive C for utilized agricultural areas and the TWI with the classes in which landslides are most likely to occur, ranging from 4 to 8 (Table 1).

3.2. Susceptibility Map and Validation

The summation of the C of all causal factors (slope, aspect, extreme precipitation, NDVI, lithology, CLC, TWI), representing layers in a GIS environment, allowed the definition of a landslide susceptibility map. The values found were then rescaled to a value between 0 and 100, where 100 indicates the maximum landslide probability in that area and 0 indicates the minimum landslide probability in that area (Figure 6).

Table 1. Causal factors with division into classes and the relative positive (W^+) and negative (W^-) weight of each class, summarized in the contrast value (C).

Causal Factor	Classes	W^+	W^-	C
SLOPE	0–16°	−0.18	0.13	−0.31
	16–25°	0.35	−0.29	0.64
	25–35°	−1.18	0.03	−1.22
	>35°	−0.61	0.06	−0.66
ASPECT	FLAT (0°)	−2.40	0.04	−2.44
	NORTH (337.5–22.5°)	0.50	−0.03	0.53
	NORTH-EAST (22.5–67.5°)	0.23	−0.04	0.27
	EAST (67.5–112.5°)	0.03	−0.01	0.04
	SOUTH-EAST (112.5–157.5°)	−0.34	0.05	−0.39
	SOUTH (157.5–202.5°)	−0.46	0.04	−0.51
	SOUTH-WEST (202.5–247.5°)	−0.29	0.03	−0.32
	WEST (247.5–292.5°)	−0.01	0.00	−0.01
	NORTH-WEST (292.5–337.5°)	0.31	−0.05	0.36
EXTREME DAILY PRECIPITATION	100–115	0.23	−0.05	0.28
	115–130	−0.02	0.01	−0.02
	130–145	0.17	−0.04	0.21
	145–160	0.13	−0.02	0.15
	160–175	−0.12	0.01	−0.14
	175–190	−0.46	0.02	−0.48
	190–205	−0.78	0.03	−0.81
	205–250	−1.59	0.03	−1.61
NDVI	−1 to 0.2	0.61	−0.00	0.61
	0.2 to 0.5	0.05	−0.02	0.07
	0.5 to 1	−0.03	0.06	−0.09
LITHOLOGY	Clays and marly clays with intercalations of sandstone, sands and conglomerates	−0.08	0.01	−0.09
	Deposits	0.34	−0.39	0.73
	Limestones, flinty limestones, subordinately marls and clay marls	−1.20	0.11	−1.32
	Marls, clay marls and marly limestones	−0.31	0.02	−0.33
	Sandstones, marly clays, subordinately conglomerates	−0.48	0.06	−0.54
	Shales and marls encompassing calcareous, marly limestones and arenaceous bodies	−1.54	0.01	−1.55
CLC	Artificial surface	−1.32	0.04	−1.36
	Agricultural surface used	0.21	−0.49	0.69
	Semi-natural wooded territories	−0.40	0.15	−0.54
	Water bodies	−1.41	0.00	−1.41
TWI	0–2	−3.46	0.00	−3.46
	2–4	−0.58	0.03	−0.60
	4–6	0.11	−0.11	0.23
	6–8	0.07	−0.04	0.11
	8–10	−0.01	−0.01	−0.01
	10–12	−0.49	0.01	−0.50
	12–23	−1.14	0.02	−1.16

The class with the largest area is the 70–80 class, with a total area of 2896.69 km^2, while the class with the smallest area is the 0–10 class, with a total area of 0.03 km^2; the largest LSI, indicated by the 90–100 class, has an area of 393.94 km^2, which corresponds to 4.21% of the entire study area (Table 2).

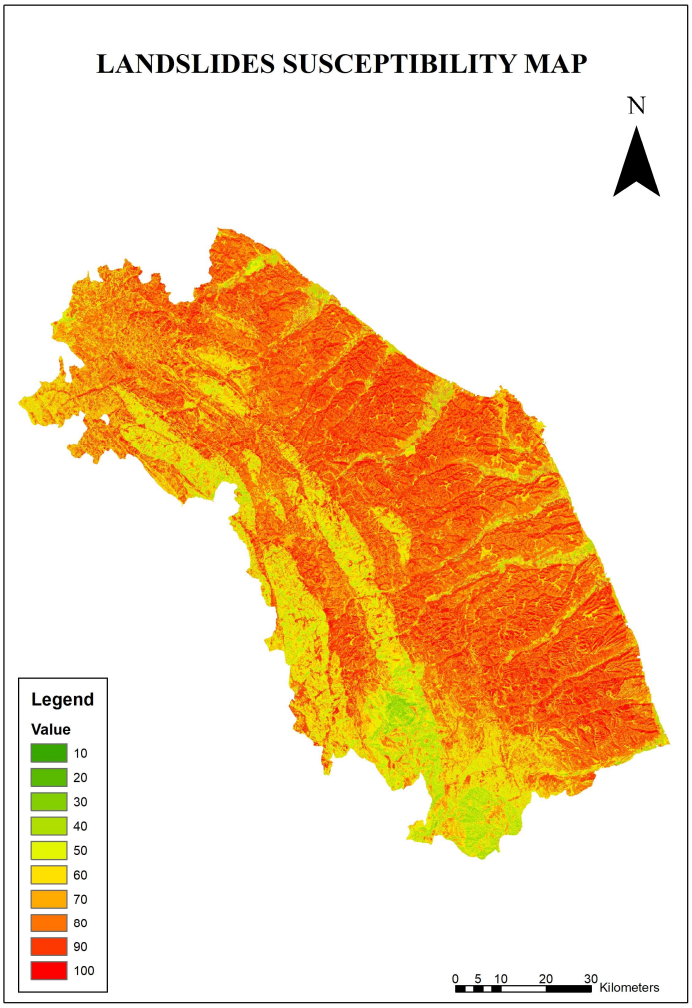

Figure 6. Landslide susceptibility map with values between 0 and 100.

Table 2. Landslide susceptibility index in relation to the area.

Value	Area (km^2)	Area (%)
0–10	0.03	0.0003
10–20	1.75	0.0187
20–30	48.16	0.5150
30–40	392.84	4.2006
40–50	780.72	8.3483
50–60	1165.00	12.4573
60–70	1678.68	17.9502
70–80	2896.69	30.9743
80–90	1994.09	21.3228
90–100	393.94	4.2125

Therefore, according with the scientific literature, the landslides susceptibility map are divided into five classes: very low, low, moderate, high and very high [51].

As a result, the territory of this region has quite pronounced hydrogeological instability (Figure 7). Obviously, although the class division performed finds some analogues in the scientific literature on the subject, it is questionable and subject to subjective evaluations that could redefine the qualitative classification of landslide probability. In any case, our assessment shows that only approximately 26% of the territory has a low or moderate probability of generating a landslide, which therefore tends to exclude serious slope instability in those areas (Table 3).

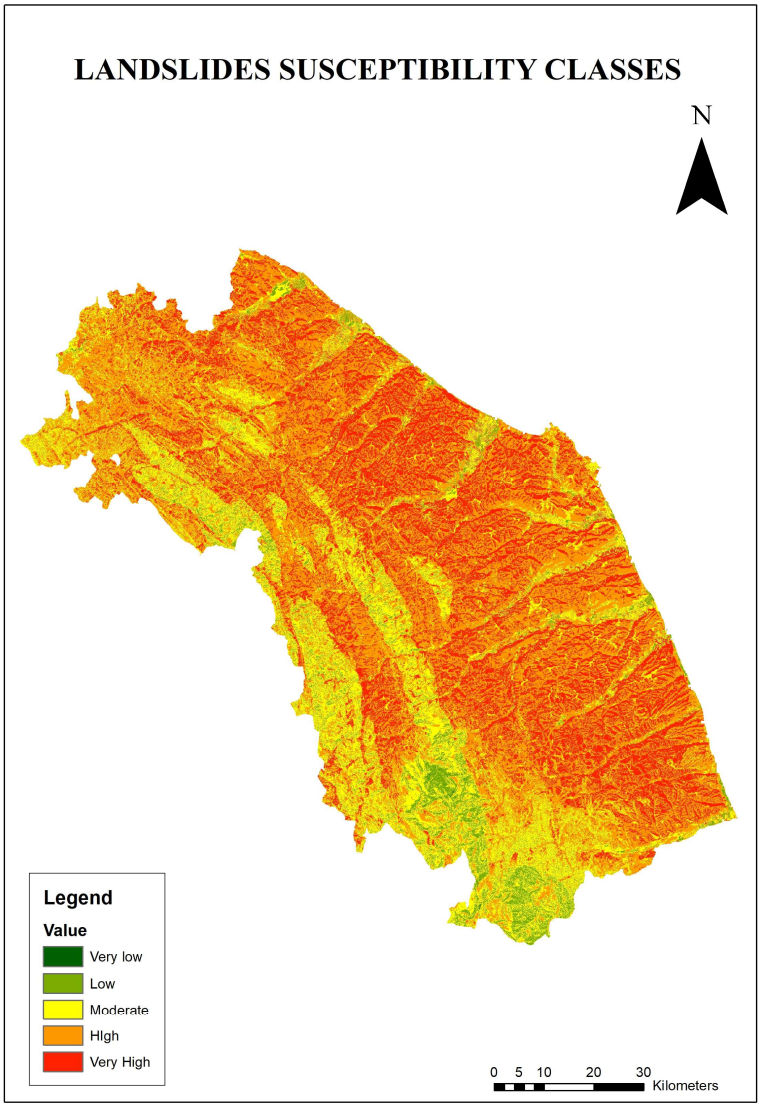

Figure 7. Landslide susceptibility classes.

Table 3. Landslide Susceptibility index in relation to the area.

Probability of Landslide	Area (km^2)	Area (%)
Very low (0–28)	1.78	0.02
Low (28–46)	444.00	4.72
Moderate (46–64)	1945.72	20.81
High (64–82)	4575.37	48.92
Very high (82–100)	2388.04	25.54

After producing the landslide susceptibility map, the AUC method was chosen as the validation method to verify the reliability of the model. In summary, validation is important because it allows us to verify the accuracy of the model used for the landslide susceptibility map and to identify any problems or limitations so that it can be improved and made more accurate. The AUC calculation was performed by taking 20% of the landslides used for the susceptibility map as training data. As described in the method, the ROC curve was prepared by superimposing the validation landslides on the LSI map. This validation procedure showed that the area under the curve was 0.75 (Figure 8); therefore, it is a moderately accurate model.

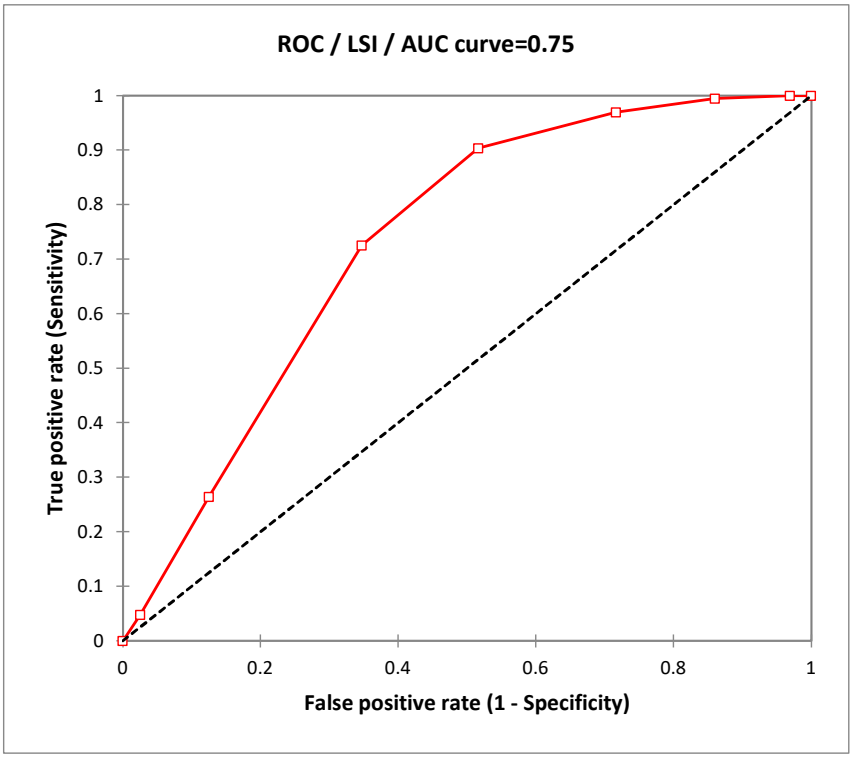

Figure 8. Validation of the model with the ROC curve.

The *Y*-axis of the curve represents the true-positive rate (i.e., success rate), which indicates the "correct prediction" of the cumulative percentage of landslide area derived from the model relative to the total landslide area in each factor class interval. The *X*-axis of the curve represents the false positive rate (1-specificity), which indicates the ratio of the cumulative non-landslide area to the total non-landslide area in each factor class interval (Figure 8).

4. Discussion

The area analyzed by this study is rather large, a good 9344 km^2 for the application of a statistical method aimed at analyzing the landslide susceptibility of the territory. Moreover, there is a very high degree of inhomogeneity in terms of vegetation, geological and morphological characteristics, which makes the generalization of the areas more complicated, also in light of the many landslides surveyed, more than 14,000. In fact, very often similar research conducted with statistical methods and in some cases with the WoE are carried out on smaller territories with an analysis of far fewer landslide events [2,52–55]. The analysis of a contained area inevitably leads to better results in the detection of probable landslide areas, precisely because one is in a more homogenous territory that therefore has similar characteristics throughout its extension. In this case, a very complex problem was faced, namely that of finding a valid model for large and diverse territories, which nevertheless gave good results with an AUC of 0.75 and allows an analysis on a decidedly larger scale also on the basis of the causal factors chosen. In some cases, much smaller study areas show worse or similar validation results to those found in this research [56–58], although many cases show better performance, but always within much smaller areas, very often on a basin scale [59–61]. Obviously, it is the chosen causal factors that lead to the results of this study in addition to the statistical method used and the use of GIS software for layer representation and map creation. In general, the scientific literature agrees that lithological characteristics are crucial for the calculation of susceptibility because they profoundly influence soil stability, and different lithological units have different landslide susceptibilities, as also shown in this study [62,63]. There are also other parameters that are routinely considered in the scientific literature on the subject, such as slope gradient, but

also exposure, in this case there were discriminatory results for the various classes and in agreement with what is to be expected. In particular, inclinations between 16 and 25 degrees were found to be the most likely to accommodate landslide movements, as were slopes facing predominantly North. In the literature while it is easy to find correspondences with slope grades and with similar degrees of acclivity to the present study, good performance is not always found in the case of slope exposure, although when significant the North is the direction most prone to landslide movements [64,65]. Among these causal factors, TWI can also be considered topographical, as it allows the quantification of topographical control over hydrological processes [40]. In the literature and in some cases, especially on much smaller areas than the one under study here, TWI shows a directly proportional relationship with landsliding, although in this case only values between 4 and 8 [66]. Most studies take geological and geomorphological causal factors into account, to the exclusion of others such as vegetational and climatic ones [67]. In particular, it has been scientifically proven that extreme precipitation events increase the possibility of a landslide triggering [68,69]. In this study, the weight of extreme precipitation is probably partly obscured by the fact that the most intense precipitation occurs in the mountainous area, which is not a prevalent location for the landslide movements studied [70]. Finally, the last two indices, one the CLC, which allows land use to be taken into account in the analysis of landslide susceptibility, while the other the NDVI relates to vegetation. The CLC is widely used in the literature and always with good results, showing as in the present study that the areas most prone to landslides are those related to agricultural soils used [24,71]. NDVI is also a widely used causal factor; however, in this case, it was used averaged over many years, instead of a few frames hypothetically describing the seasonal trend [72]. The NDVI showed a great effect on landslide susceptibility showing rather high weights in bare soils, similar to what can be observed in the more recent scientific literature [73].

5. Conclusions

This paper represents a model for the analysis of landslide susceptibility over large areas, in particular, the causal factors chosen lend themselves to an interpretation that provides good results, in terms of AUC compared to the existing literature on the topic, especially in relation to the area of over 9000 km^2 analyzed. Topographical, land-use, climatic, and vegetation parameters were considered, with weights that discriminated in most cases those classes that are also identified as more prone to landslide movements in the literature. The database used was very large, but also reliable and allowed for a detailed analysis of landslide movements, even over such a large area as the one analyzed. The WoE method has proven to be very reliable (AUC = 0.75), as it is based on the analysis of layers (causal factors) that overlap the landslide map, and this especially with such a large database allows very good discrimination of features contributing to triggering. However, similar to any research, there is a margin for improvement that would be interesting to explore and that could further improve the already good value obtained from validation through the AUC method. First, it has been observed in the scientific literature that WoE, similar to most statistical methods, obtains the best results in the case of homogeneous environments, so it might be interesting to subdivide the territory, on elevation or lithological bands, to be analyzed separately; this would determine for large spatial extensions two or more models that would work with different but more accurate results for individual isolated areas, thus with different weights for the causal factors. Second, the resolution of NDVI could be improved and raised from 250 m to much lower values although it would be much more complicated to handle hundreds of satellite images. In addition, the consideration made to improve the WoE could also improve the significance of extreme precipitation weights, which could be differentiated according to homogeneous areas. In conclusion, it is crucial to provide institutions with increasingly reliable and high-performing susceptibility analysis tools in order to be able to choose the areas on which to intervene before disasters involving property and especially people occur.

Author Contributions: Conceptualization, M.G.; methodology, M.G.; software, N.P.; validation, M.G. and G.P.; formal analysis, N.P.; investigation, N.P. and A.R.; resources, M.G.; data curation, G.P.; writing—original draft preparation, M.G.; writing—review and editing, M.G.; visualization, M.G. and A.D.; supervision, G.P.; project administration, G.P. All authors have read and agreed to the published version of the manuscript.

Funding: This research received no external funding.

Institutional Review Board Statement: Not applicable.

Informed Consent Statement: Not applicable.

Data Availability Statement: Landslides (https://www.autoritadistrettoac.it/pianificazione/bacino-idrografico/bacini-marchigiani/cartografia-pai-marche accessed on 20 March 2023). Geological map (https://www.regione.marche.it/Regione-Utile/PaesaggioTerritoryUrbanPlanning/Cartography/Repertoire/Cartotageologicaregionale10000 accessed on 20 March 2023). CLC (https://groupware.sinanet.isprambiente.it/uso-copertura-e-consumo-di-suolo/library/copertura-del-suolo/corine-land-cover/clc2018_shapefile accessed on 20 March 2023). NDVI (https://appeears.earthdatacloud.nasa.gov/view/b42ca867-084d-4602-ab01-b8065a148645 accessed on 20 March 2023).

Conflicts of Interest: The authors declare no conflict of interest.

References

1. Trigila, A.; Iadanza, C.; Bussettini, M.; Lastoria, B. *Dissesto Idrogeologico in Italia: Pericolosità e Indicatori di Rischio-Edizione 2018*; ISPRA: Roma, Italy, 2018.
2. Reichenbach, P.; Rossi, M.; Malamud, B.D.; Mihir, M.; Guzzetti, F. A review of statistically-based landslide susceptibility models. *Earth-Sci. Rev.* **2018**, *180*, 60–91. [CrossRef]
3. Deng, X.; Li, L.; Tan, Y. Validation of spatial prediction models for landslide susceptibility mapping by considering structural similarity. *ISPRS Int. J. Geo-Inf.* **2017**, *6*, 103. [CrossRef]
4. Dou, J.; Oguchi, T.; Hayakawa, Y.S.; Uchiyama, S.; Saito, H.; Paudel, U. GIS-based landslide susceptibility mapping using a certainty factor model and its validation in the Chuetsu Area, Central Japan. In *Landslide Science for a Safer Geoenvironment, Volume 2: Methods of Landslide Studies*; Springer International Publishing: Berlin/Heidelberg, Germany, 2014; Volume 2, pp. 419–424.
5. Akgun, A.; Erkan, O. Landslide susceptibility mapping by geographical information system-based multivariate statistical and deterministic models: In an artificial reservoir area at Northern Turkey. *Arab. J. Geosci.* **2016**, *9*, 1–15. [CrossRef]
6. Jia, N.; Mitani, Y.; Xie, M.; Djamaluddin, I. Shallow landslide hazard assessment using a three-dimensional deterministic model in a mountainous area. *Comput. Geotech.* **2012**, *45*, 1–10. [CrossRef]
7. Chen, L.K.; Chang, C.H.; Liu, C.H.; Ho, J.Y. Application of a three-dimensional deterministic model to assess potential landslides, a case study: Antong Hot Spring Area in Hualien, Taiwan. *Water* **2020**, *12*, 480. [CrossRef]
8. Huang, J.C.; Kao, S.J.; Hsu, M.L.; Lin, J.C. Stochastic procedure to extract and to integrate landslide susceptibility maps: An example of mountainous watershed in Taiwan. *Nat. Hazards Earth Syst. Sci.* **2006**, *6*, 803–815. [CrossRef]
9. Ciurleo, M.; Cascini, L.; Calvello, M. A comparison of statistical and deterministic methods for shallow landslide susceptibility zoning in clayey soils. *Eng. Geol.* **2017**, *223*, 71–81. [CrossRef]
10. Montgomery, D.R.; Dietrich, W.E. A physically based model for the topographic control on shallow landsliding. *Water Resour. Res.* **1994**, *30*, 1153–1171. [CrossRef]
11. Pradhan, A.M.S.; Kim, Y.T. Evaluation of a combined spatial multi-criteria evaluation model and deterministic model for landslide susceptibility mapping. *Catena* **2016**, *140*, 125–139. [CrossRef]
12. Cascini, L. Applicability of landslide susceptibility and hazard zoning at different scales. *Eng. Geol.* **2008**, *102*, 164–177. [CrossRef]
13. Fell, R.; Corominas, J.; Bonnard, C.; Cascini, L.; Leroi, E.; Savage, W.Z. Guidelines for landslide susceptibility, hazard and risk zoning for land use planning. *Eng. Geol.* **2008**, *102*, 85–98. [CrossRef]
14. Vergari, F.; Della Seta, M.; Del Monte, M.; Fredi, P.; Lupia Palmieri, E. Landslide susceptibility assessment in the Upper Orcia Valley (Southern Tuscany, Italy) through conditional analysis: A contribution to the unbiased selection of causal factors. *Nat. Hazards Earth Syst. Sci.* **2011**, *11*, 1475–1497. [CrossRef]
15. Aditian, A.; Kubota, T.; Shinohara, Y. Comparison of GIS-based landslide susceptibility models using frequency ratio, logistic regression, and artificial neural network in a tertiary region of Ambon, Indonesia. *Geomorphology* **2018**, *318*, 101–111. [CrossRef]
16. Juliev, M.; Mergili, M.; Mondal, I.; Nurtaev, B.; Pulatov, A.; Hübl, J. Comparative analysis of statistical methods for landslide susceptibility mapping in the Bostanlik District, Uzbekistan. *Sci. Total Environ.* **2019**, *653*, 801–814. [CrossRef]
17. Kayastha, P.; Dhital, M.R.; De Smedt, F. Landslide susceptibility mapping using the weight of evidence method in the Tinau watershed, Nepal. *Nat. Hazards* **2012**, *63*, 479–498. [CrossRef]
18. Cao, Y.; Wei, X.; Fan, W.; Nan, Y.; Xiong, W.; Zhang, S. Landslide susceptibility assessment using the Weight of Evidence method: A case study in Xunyang area, China. *PLoS ONE* **2021**, *16*, e0245668. [CrossRef] [PubMed]

19. Duman, T.Y.; Can, T.; Gokceoglu, C.; Nefeslioglu, H.A.; Sonmez, H. Application of logistic regression for landslide susceptibility zoning of Cekmece Area, Istanbul, Turkey. *Environ. Geol.* **2006**, *51*, 241–256. [CrossRef]
20. Onagh, M.; Kumra, V.K.; Rai, P.K. Landslide susceptibility mapping in a part of Uttarkashi district (India) by multiple linear regression method. *Int. J. Geol. Earth Environ. Sci.* **2012**, *2*, 102–120.
21. Pradhan, B. Use of GIS-based fuzzy logic relations and its cross application to produce landslide susceptibility maps in three test areas in Malaysia. *Environ. Earth Sci.* **2011**, *63*, 329–349. [CrossRef]
22. Van Dao, D.; Jaafari, A.; Bayat, M.; Mafi-Gholami, D.; Qi, C.; Moayedi, H.; Van Phong, T.; Ly, H.B.; Le, T.T.; Trinh, P.T.; et al. A spatially explicit deep learning neural network model for the prediction of landslide susceptibility. *Catena* **2020**, *188*, 104451.
23. Saleem, N.; Huq, M.E.; Twumasi, N.Y.D.; Javed, A.; Sajjad, A. Parameters derived from and/or used with digital elevation models (DEMs) for landslide susceptibility mapping and landslide risk assessment: A review. *ISPRS Int. J. Geo-Inf.* **2019**, *8*, 545. [CrossRef]
24. Günther, A.; Van Den Eeckhaut, M.; Malet, J.P.; Reichenbach, P.; Hervás, J. Climate-physiographically differentiated Pan-European landslide susceptibility assessment using spatial multi-criteria evaluation and transnational landslide information. *Geomorphology* **2014**, *224*, 69–85. [CrossRef]
25. Gentilucci, M.; Materazzi, M.; Pambianchi, G. Statistical Analysis of Landslide Susceptibility, Macerata Province (Central Italy). *Hydrology* **2021**, *8*, 5. [CrossRef]
26. Pourghasemi, H.R.; Pradhan, B.; Gokceoglu, C.; Deylami Moezzi, K. Landslide susceptibility mapping using a spatial multi criteria evaluation model at Haraz Watershed, Iran. In *Terrigenous Mass Movements: Detection, Modelling, Early Warning and Mitigation Using Geoinformation Technology*; Springer: Berlin/Heidelberg, Germany, 2012; pp. 23–49.
27. Gentilucci, M.; Barbieri, M.; Materazzi, M.; Pambianchi, G. Effects of Climate Change on Vegetation in the Province of Macerata (Central Italy). In *Advanced Studies in Efficient Environmental Design and City Planning*; Springer International Publishing: Berlin/Heidelberg, Germany, 2021; pp. 463–474.
28. Conoscenti, C.; Agnesi, V.; Angileri, S.; Cappadonia, C.; Rotigliano, E.; Märker, M. A GIS-based approach for gully erosion susceptibility modelling: A test in Sicily, Italy. *Environ. Earth Sci.* **2013**, *70*, 1179–1195. [CrossRef]
29. Cervi, F.; Berti, M.; Borgatti, L.; Ronchetti, F.; Manenti, F.; Corsini, A. Comparing predictive capability of statistical and deterministic methods for landslide susceptibility mapping: A case study in the northern Apennines (Reggio Emilia Province, Italy). *Landslides* **2010**, *7*, 433–444. [CrossRef]
30. Nsengiyumva, J.B.; Luo, G.; Amanambu, A.C.; Mind'je, R.; Habiyaremye, G.; Karamage, F.; Ochege, F.U.; Mupenzi, C. Comparing probabilistic and statistical methods in landslide susceptibility modeling in Rwanda/Centre-Eastern Africa. *Sci. Total Environ.* **2019**, *659*, 1457–1472. [CrossRef]
31. Do, H.M.; Yin, K.L.; Guo, Z.Z. A comparative study on the integrative ability of the analytical hierarchy process, weights of evidence and logistic regression methods with the Flow-R model for landslide susceptibility assessment. *Geomat. Nat. Hazards Risk* **2020**, *11*, 2449–2485. [CrossRef]
32. Othman, A.A.; Gloaguen, R.; Andreani, L.; Rahnama, M. Improving landslide susceptibility mapping using morphometric features in the Mawat area, Kurdistan Region, NE Iraq: Comparison of different statistical models. *Geomorphology* **2018**, *319*, 147–160. [CrossRef]
33. Gentilucci, M.; Barbieri, M.; Pambianchi, G. Reliability of the IMERG product through reference rain gauges in Central Italy. *Atmos. Res.* **2022**, *278*, 106340. [CrossRef]
34. Gentilucci, M.; Barbieri, M.; Dalei, N.N.; Gentilucci, E. Management and Creation of a New Tourist Route in the National Park of the Sibillini Mountains using GIS Software, for Economic Development. In Proceedings of the GISTAM, Heraklion, Greece, 3–5 May 2019; pp. 183–188.
35. Coltorti, M.; Farabollini, P.; Gentili, B.; Pambianchi, G. Geomorphological evidence for anti-Apennine faults in the Umbro-Marchean Apennines and in the peri-Adriatic basin, Italy. *Geomorphology* **1996**, *15*, 33–45. [CrossRef]
36. Bisci, C.; Dramis, F. Il concetto di attività in geomorfologia: Problemi e metodi di valutazione. *Geogr. Fis. Dinam. Quat.* **1991**, *14*, 193–199.
37. Gentilucci, M.; Barbieri, M.; Lee, H.S.; Zardi, D. Analysis of rainfall trends and extreme precipitation in the Middle Adriatic Side, Marche Region (Central Italy). *Water* **2019**, *11*, 1948. [CrossRef]
38. Gentilucci, M.; Burt, P. Using temperature to predict the end of flowering in the common grape (Vitis vinifera) in the Macerata wine region, Italy. *Euro-Mediterr. J. Environ. Integr.* **2018**, *3*, 38. [CrossRef]
39. Bonham-Carter, G.F.; Agterberg, F.P.; Wright, D.F. Integration of geological datasets for gold exploration in Nova Scotia. *Digit. Geol. Geogr. Inf. Syst.* **1989**, *10*, 15–23.
40. Barbieri, G.; Cambuli, P. The weight of evidence statistical method in landslide susceptibility mapping of the Rio Pardu Valley (Sardinia, Italy). In Proceedings of the 18th World IMACS Congress and MODSIM09 International Congress on Modelling and Simulation: Interfacing Modelling and Simulation with Mathematical and Computational Sciences, Cairns, Australia, 13–17 July 2009; pp. 2658–2664.
41. Regmi, N.R.; Giardino, J.R.; Vitek, J.D. Modeling susceptibility to landslides using the weight of evidence approach: Western Colorado, USA. *Geomorphology* **2010**, *115*, 172–187. [CrossRef]
42. Anbalagan, R. Landslide hazard evaluation and zonation mapping in mountainous terrain. *Eng. Geol.* **1992**, *32*, 269–277. [CrossRef]

43. Sörensen, R.; Zinko, U.; Seibert, J. On the calculation of the topographic wetness index: Evaluation of different methods based on field observations. *Hydrol. Earth Syst. Sci.* **2006**, *10*, 101–112. [CrossRef]
44. Aringoli, D.; Farabollini, P.; Gentili, B.; Materazzi, M.; Pambianchi, G. Examples of geoparks and geoconservation strategies from the Southern Umbro-Marchean Apennines (Central Italy). *GeoActa* **2010**, *3*, 153–166.
45. Bharathkumar, L.; Mohammed-Aslam, M.A. Crop pattern mapping of tumkur taluk using NDVI technique: A remote sensing and GIS approach. *Aquat. Procedia* **2015**, *4*, 1397–1404. [CrossRef]
46. Wubalem, A.; Meten, M. Landslide susceptibility mapping using information value and logistic regression models in Goncha Siso Eneses area, northwestern Ethiopia. *SN Appl. Sci.* **2020**, *2*, 807. [CrossRef]
47. Goodenough, D.J.; Rossmann, K.; Lusted, L.B. Radiographic applications of receiver operating characteristic (ROC) curves. *Radiology* **1974**, *110*, 89–95. [CrossRef]
48. Adams, N.M.; Hand, D.J. Comparing classifiers when the misallocation costs are uncertain. *Pattern Recognit.* **1999**, *32*, 1139–1147. [CrossRef]
49. Hanley, J.A.; McNeil, B.J. The meaning and use of the area under a receiver operating characteristic (ROC) curve. *Radiology* **1982**, *143*, 29–36. [CrossRef] [PubMed]
50. Swets, J.A. Measuring the accuracy of diagnostic systems. *Science* **1988**, *240*, 1285–1293. [CrossRef] [PubMed]
51. Getachew, N.; Meten, M. Weights of evidence modeling for landslide susceptibility mapping of Kabi-Gebro locality, Gundomeskel area, Central Ethiopia. *Geoenviron. Disasters* **2021**, *8*, 1–22. [CrossRef]
52. Ilia, I.; Tsangaratos, P. Applying weight of evidence method and sensitivity analysis to produce a landslide susceptibility map. *Landslides* **2016**, *13*, 379–397. [CrossRef]
53. Lee, S.; Choi, J. Landslide susceptibility mapping using GIS and the weight-of-evidence model. *Int. J. Geogr. Inf. Sci.* **2004**, *18*, 789–814. [CrossRef]
54. Vakhshoori, V.; Zare, M. Landslide susceptibility mapping by comparing weight of evidence, fuzzy logic, and frequency ratio methods. *Geomat. Nat. Hazards Risk* **2016**, *7*, 1731–1752. [CrossRef]
55. Gomez, H.; Kavzoglu, T. Assessment of shallow landslide susceptibility using artificial neural networks in Jabonosa River Basin, Venezuela. *Eng. Geol.* **2005**, *78*, 11–27. [CrossRef]
56. Nicu, I.C. Frequency ratio and GIS-based evaluation of landslide susceptibility applied to cultural heritage assessment. *J. Cult. Herit.* **2017**, *28*, 172–176. [CrossRef]
57. Panahi, M.; Rahmati, O.; Rezaie, F.; Lee, S.; Mohammadi, F.; Conoscenti, C. Application of the group method of data handling (GMDH) approach for landslide susceptibility zonation using readily available spatial covariates. *Catena* **2022**, *208*, 105779. [CrossRef]
58. Schicker, R.; Moon, V. Comparison of bivariate and multivariate statistical approaches in landslide susceptibility mapping at a regional scale. *Geomorphology* **2012**, *161*, 40–57. [CrossRef]
59. Chen, W.; Xie, X.; Peng, J.; Shahabi, H.; Hong, H.; Bui, D.T.; Duan, Z.; Li, S.; Zhu, A.X. GIS-based landslide susceptibility evaluation using a novel hybrid integration approach of bivariate statistical based random forest method. *Catena* **2018**, *164*, 135–149. [CrossRef]
60. Conoscenti, C.; Rotigliano, W.; Cama, M.; Almaru Caraballo-Arias, N.; Lombardo, L.; Agnesi, V. Exploring the effect of absence selection on landslide susceptibility models: A case study in Sicily, Italy. *Geomorphology* **2016**, *261*, 222–235. [CrossRef]
61. Jia, W.; Wen, T.; Li, D.; Guo, W.; Quan, Z.; Wang, Y.; Huang, D.; Hu, M. Landslide Displacement Prediction of Shuping Landslide Combining PSO and LSSVM Model. *Water* **2023**, *15*, 612. [CrossRef]
62. Dai, F.C.; Lee, C.F.; Li, J.; Xu, Z.W. Assessment of landslide susceptibility on the natural terrain of Lantau Island, Hong Kong. *Environ. Geol.* **2001**, *40*, 381–391.
63. Caniani, D.; Pascale, S.; Sdao, F.; Sole, A. Neural networks and landslide susceptibility: A case study of the urban area of Potenza. *Nat. Hazards* **2008**, *45*, 55–72. [CrossRef]
64. Armaş, I. Weights of evidence method for landslide susceptibility mapping. Prahova Subcarpathians, Romania. *Nat. Hazards* **2012**, *60*, 937–950. [CrossRef]
65. Baeza, C.; Corominas, J. Assessment of shallow landslide susceptibility by means of multivariate statistical techniques. *Earth Surf. Process. Landf. J. Br. Geomorphol. Res. Group* **2001**, *26*, 1251–1263. [CrossRef]
66. Pourghasemi, H.R.; Kornejady, A.; Kerle, N.; Shabani, F. Investigating the effects of different landslide positioning techniques, landslide partitioning approaches, and presence-absence balances on landslide susceptibility mapping. *Catena* **2020**, *187*, 104364. [CrossRef]
67. Ayalew, L.M.; Yamagishi, H. The application of GIS-based logistic regression for landslide susceptibility mapping in the Kakuda-Yahiko Mountains, Central Japan. *Geomorphology* **2005**, *65*, 15–31. [CrossRef]
68. Clarke, M.L.; Rendell, H.M. Process–form relationships in Southern Italian badlands: Erosion rates and implications for landform evolution. *Earth Surf. Process. Landf. J. Br. Geomorphol. Res. Group* **2006**, *31*, 15–29. [CrossRef]
69. Papathoma-Koehle, M.; Keiler, M.; Totschnig, R.; Glade, T. Improvement of vulnerability curves using data from extreme events: Debris flow event in South Tyrol. *Nat. Hazards* **2012**, *64*, 2083–2105. [CrossRef]
70. Soldini, L.; Darvini, G. Extreme rainfall statistics in the Marche region, Italy. *Hydrol. Res.* **2017**, *48*, 686–700. [CrossRef]
71. Meneses, B.M.; Pereira, S.; Reis, E. Effects of different land use and land cover data on the landslide susceptibility zonation of road networks. *Nat. Hazards Earth Syst. Sci.* **2019**, *19*, 471–487. [CrossRef]

72. Chen, W.; Li, Y. GIS-based evaluation of landslide susceptibility using hybrid computational intelligence models. *Catena* **2020**, *195*, 104777. [CrossRef]
73. Lee, S.; Talib, J.A. Probabilistic landslide susceptibility and factor effect analysis. *Environ. Geol.* **2005**, *47*, 982–990. [CrossRef]